

# HIGH FREQUENCY MULTIPURPOSE SiC MOSFET DRIVER

Jan STROSSA , Vladislav DAMEC , Martin SOBEK , Daniel KOURIL , Jakub BACA 

Department of Electronics, Faculty of Electrical Engineering and Computer Science,  
VSB–Technical University of Ostrava, 17. listopadu 2172/15, 708 00 Ostrava, Czech Republic

jan.strossa@vsb.cz, vladislav.damec@vsb.cz, martin.sobek@vsb.cz, daniel.kouril@vsb.cz, jakub.baca@vsb.cz

DOI: 10.15598/aeec.v19i3.4159

Article history: Received Mar 11, 2021; Revised Apr 24, 2021; Accepted May 12, 2021; Published Sep 30, 2021.  
This is an open access article under the BY-CC license.

**Abstract.** *This article describes a new multipurpose Silicon-Carbide (SiC) Metal Oxide Semiconductor Field Effect Transistor (MOSFET) driver, which was designed and manufactured for a high frequency operating SiC transistor as a semiconductor switching device of power converters. The design of the introduced driver enables to adjust the output voltage levels easily by choosing the integrated linear voltage stabilizers with suitable output parameters used for Printed Circuit Board (PCB) mounting. The voltage insulation of the proposed driver between the primary control side and the secondary output side is performed by MGJ6D12H24MC muRata Ps DC-DC converter with a declared  $dv/dt$  immunity 80 kV/1000 ms at 1.6 kV and by IX3180 IXYS High Speed gate driver optocouplers with a declared 10 kV/1000 ms minimum common mode rejection at 1.5 kV. The voltage insulation of these coupling elements is accompanied by safety gaps on the PCB. These insulation features enable the proposed driver to work on high frequencies as a high-side transistor of H-bridges as same as in other power converter topologies with a high frequency and high voltage stress of the insulation border. The proposed driver also provides the possibility of tripping the signal, when the short circuit of the controlled power transistor occurs.*

## Keywords

*Driver, high switching frequency, MOSFET, multipurpose driver, overshoot, SiC.*

## 1. Introduction

Modern Silicon-Carbide (SiC) Metal Oxide Semiconductor Field Effect Transistors (MOSFET) can be used in power converter applications working with high switching frequencies in a range from tens of kHz up to MHz. High switching frequency with a combination of low transistor switching charge brings a possibility of fast switching with low power losses [1] and [2]. This leads to low switching losses due to fast transistor opening and closing and low consumed power for control the transistor due to low gate charge [3] and [4].

The requirements for a precise gate-source voltage control arise from accomplish the precise switching stated above [5]. Fast rise and fall times of the gate-source voltage are necessary for a fast switching and related low switching loss achievement [6]. The related fast switching enables the converter to work with high control dynamics, which is often required within control algorithms [7]. The steady levels of the gate-source voltage, mainly the positive level of the switched-on state, are demanded to be close to the maximum rating values of the used power transistor to eliminate the conduction and leakage losses [8]. These requirements originate especially in a necessity of precise tune up the driver output resistance in high voltage converter applications. It is caused by the wave impedance of the cable line applied between the driver and controlled transistor and the transistor input capacity [9], [10], and [11]. This adjustment is usually necessary because of the gate-source voltage overshoot originated at the end of the control signal rising edge and the falling edge, respectively. Generally, it is demanded to develop a multipurpose driver adjustable for the specific application.

The high voltage stress of insulation border between the primary and secondary parts of the driver is orig-

inated in some applications. That can be seen especially in H-bridges where the power transistor is drain connected to the steady point of power voltage with reference to the control system ground. This voltage stress is more strenuous with a faster switching and higher switched voltage due to capacity current flowing via the insulation border and stressing the isolating dielectric.

In general, relatively high switching frequencies and related fast rise and fall times of switched semiconductors are achievable with the modern MOSFETs. However, it means precisely tune up the driver buffer output resistivity according to the output cable inductance, the MOSFET input capacity, and the related gate-source voltage overshoot. The overshoot is higher with a higher rising and falling gate-source voltage slopes. High switching frequencies of the applications, where the transistor source terminal changes its electric potential with changing the switch state means high insulation border stress. In general, many drivers are commercially available, and many driver designs were already published, see [12], [13], [14], [15], [16], [17], [18], [19], and [20].

The goal of the paper is to present a multipurpose driver concept with a few novel potentials according to the following specific application requirements:

- easy setup of the steady on and off state output voltage levels,
- easy setup of the output resistance to tune it up according to the output cable impedance,
- high  $dv/dt$  insulation border immunity up to  $1.7 \text{ kV} \cdot \mu\text{s}^{-1}$ ,
- signal trip extension,
- extension of transferring the information about drain-source voltage presence,
- possibility to use the device not as a transistor driver, but as an insulated voltage detector.

All the mentioned features should be feasible by choosing the appropriate PCB assembly. This makes the driver easy to release for a specific application. Moreover, it represses the risk of malfunction of less reliable parts, such as potentiometers. These parts are not used in the proposed concept.

## 2. Proposed Driver Concept

### 2.1. General Description

The proposed driver PCB contains 3 ports at the primary side and a group of 3 terminals at the sec-

ondary side, each one for one MOSFET pin, see Fig. 1. The first primary port J1 contains the power supply terminals for 9.6–18 V DC with the negative pole connected to the signal ground. This port also contains an input signal for driving the controlled transistor and it is ready to trace the controlled transistor short circuit detection trip signal too.

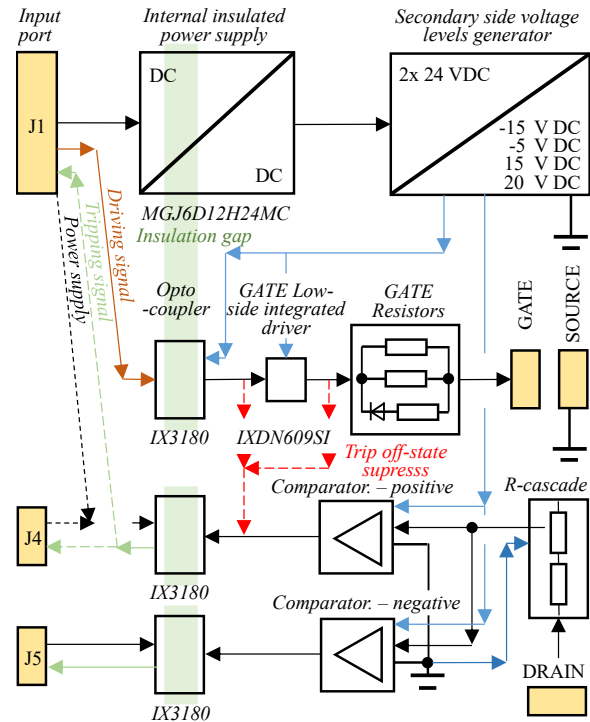


Fig. 1: Proposed driver simplified block diagram.

The next 2 primary ports contain output signals of the secondary drain-source voltage detections, port J4 reacts on positive voltage, port J5 on negative. Each of these ports has an independent power supply on the primary side, which is galvanically insulated. It can work with different voltage signal state levels according to the connected system, the voltage adjustment is possible within the choice of PCB mounting combination.

It is also possible to negate the output signal at the primary side of the positive drain-source voltage detection, which can be beneficial mainly if this signal is used as a trip function. The positive drain-source voltage detector output can be traced in the port J1 with a common signal ground as same as in port J4 with an independent ground system. In general, the positive drain-source voltage detection can be used as a trip function - in this case, the detector output is suppressed when the output transistor is in an off state. This is performed to avoid the false fault detection caused by the presence of detected voltage on the switched-off semiconductor. If the suppression is

not performed, the detector output just follows the detected voltage.

## 2.2. Secondary Side Power Supply System

The proposed concept contains a DC-DC MGJ6D12H24MC muRata Ps auxiliary source which provides the high du/dt immunity galvanic insulation of the power supply system. The unit of secondary side power supply stabilization generates 4 voltage levels, which are assumed to  $-15\text{ V}$ ,  $-5\text{ V}$ ,  $+15\text{ V}$  and  $+20\text{ V}$ , as defaults.

The levels  $\pm 15\text{ V}$  are traced onto power supplies of fast operational amplifiers, which are used as comparators within the units of drain-source voltage detections, if these functions are released. The secondary side of the driving signal optocoupler power supply is supplied asymmetrically,  $+15\text{ V}/-5\text{ V}$ , so the level  $+15\text{ V}$  is also used there. There is currently no expectation of demand to change the  $\pm 15\text{ V}$  values, but it could be demanded, e.g. in the case of the used operational amplifiers change. In this case, it can be adjusted by changing the related reference resistors series near the linear voltage regulators or by changing these regulators, which are used in the TO-252-3 and SOT-89 package, respectively. If the drain-source voltage detections are not used, PCB mounting the  $-15\text{ V}$  regulator is not necessary.

The default levels assumed as  $-5\text{ V}$ ,  $+20\text{ V}$  are used as voltages, which are switched at the gate output. These should be set according to the applied power transistor on- and off-state nominal voltage levels and the overshoot of the gate-source voltage on the applied transistor at the end of the transient switching processes.

These voltage levels are generated by the linear voltage regulators with no reference resistors and with the signal ground connected directly to the secondary ground. This ground is also connected to the transistor source potential.

The voltage regulators are used in the TO-252 package and belong to the well-known LM78xx and LM79xx series, respectively. It is necessary to set these voltage levels by choosing the appropriate voltage regulators.

The nominal off and on-state power MOSFET transistors gate-source voltages are usually asymmetrical with a lower negative level. Because of that, the secondary ground connected to the output transistor source is not connected to the middle of the DC-DC insulation auxiliary source output, even though these  $2 \times 24\text{ V}$  DC outputs are connected in series.

The secondary side ground is connected to the output of another  $-5\text{ V}$  DC linear voltage regulator, which moves the reference ground from the middle of  $2 \times 24\text{ V}$  about  $5\text{ V}$  down. This ensures that there are available c.  $+29\text{ V}$  and  $-9\text{ V}$  as the inputs for the steady state gate-source voltage regulators.

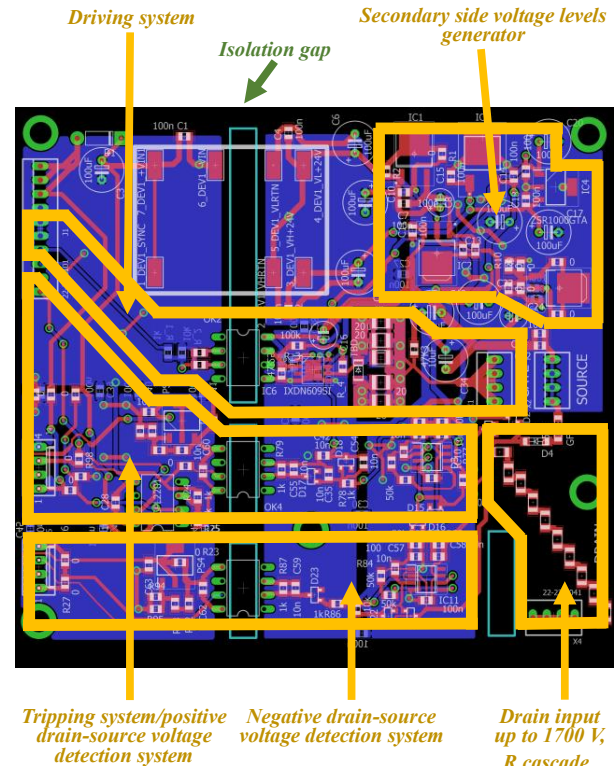


Fig. 2: Proposed driver PCB design layout, Eagle export, blue color - bottom vias, red color - top vias.

## 2.3. Driving System

The driving system contains the cascaded optocoupler IX3180, an integrated low-side MOSFET driver IXDN609SI and resistive buffer for parallel package 1210 resistors. Fast rectifying bypass diode for coupling the parallel resistors with other resistors for the negative output voltage is also installed.

The mentioned elements also contain an output to suppress the trip output to do not signalize the fail, when the power transistor is in the off-state. It is not necessary to mount parts of all the output resistors PCB pads. However, it is important to tune the total value according to the applied MOSFET and the line cable between the power transistor and the driver output [9]. It is also important to find an optimal resistors combination according to the power loss limitation of these elements.

### 2.4. Tripping System/D-S Voltage Detection

The tripping system/positive D-S voltage detector is based on the input  $R$ -cascade  $10 \times 1206$  package. This cascade couples the DRAIN input terminal, see Fig. 1, with a pair of diodes in anti-series, which ground the  $R$ -cascade via SOURCE terminal, see Fig. 1. The anti-series diodes limit the voltage between the output of the  $R$ -cascade and the system ground. This voltage is traced to comparator based on operational amplifier ADA4627. The comparison reference must be set by the related pair of resistors. The proposed PCB layout of the comparator output contains pads for placing the resistor and the capacitor for the low pass filtering at the comparator output.

The input  $R$ -cascade also originates the  $RC$  low pass filter together with diodes PN-junctions parasitic capacities. Choice of an optimal combination of input resistivity and the grounding diodes then can be used for filtering the input signal.

The main feature of the proposed positive D-S voltage detector system is the possibility of tuning up the sensitivity within a few levels. Firstly, the low pass filter originated by the input  $R$ -cascade and the related diodes can be used to suppress the noise received by the operational amplifier. Secondly, the low-pass filter, originated by the  $RC$  element of  $R_1$  and  $C_1$ , can be used to suppress some fast transient peaks at the operational amplifier output, see Fig. 3.

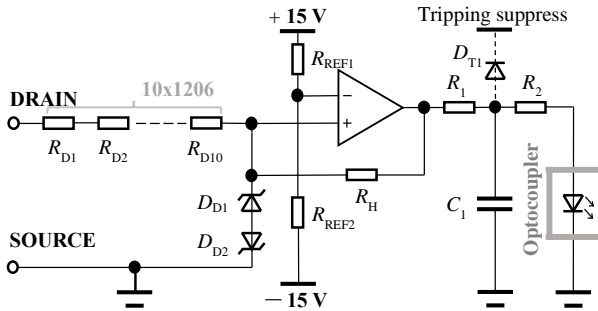


Fig. 3: Tripping system/positive D-S voltage detector system simplified circuit diagram.

Setting up the reference resistors  $R_{REF1}$  and  $R_{REF2}$  affects the reference comparison level and the input signal-to-noise ratio too.

### 3. Proposed Driver Prototype

The driver prototype was realized for driving SiC C2M0045170D MOSFET manufactured by CREE, Inc. The output resistivity was set to approximately  $3.33 \Omega$  for positive G-S voltage and  $2.22 \Omega$  for negative voltage,

using  $9 \times 20 \Omega$  resistors. The steady positive output voltage was set to  $+20 \text{ V}$ , the steady negative output voltage was set to  $-5 \text{ V}$ .

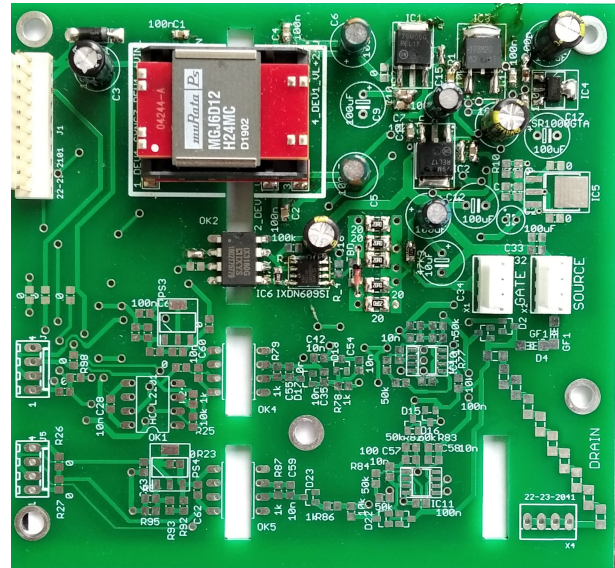


Fig. 4: Mounted proposed driver PCB.

### 4. Obtained Results

The proposed driver was applied for test onto Step-down converter based on the stated C2M0045170D MOSFET using up to  $1000 \text{ V}$  switched voltage and with the interconnection of the power transistor to the proposed driver via coaxial approximately  $20 \text{ cm}$  long cable.

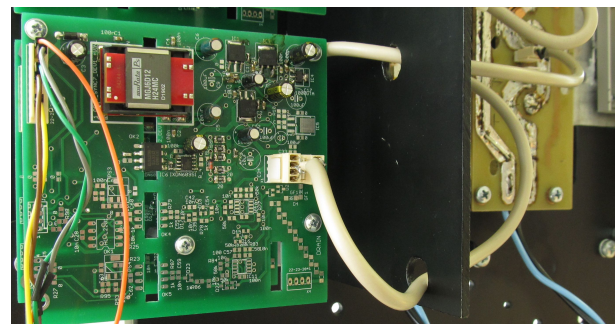


Fig. 5: Tested driver prototype application.

In Fig. 7 and Fig. 8, the responses obtained within the first driver test are presented. The test was performed without voltage at the power circuit. The switching frequency up to  $500 \text{ kHz}$  was achieved, ordinary voltage scope probes were used.

The obtained turn-on delay was approx.  $150 \text{ ns}$  and turn - off delay was approx.  $220 \text{ ns}$ , see Fig. 8. The low overshoots can be seen within the reached gate-source voltage curve, see Fig. 7 and Fig. 8.

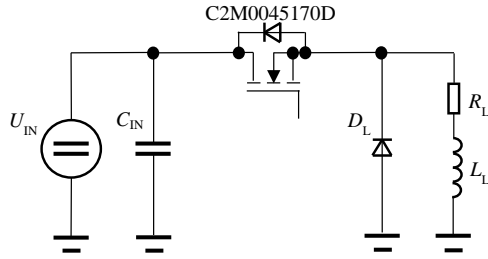


Fig. 6: Testing power circuit diagram.

capacitance of the used C2M0045170D MOSFET is 171 pF. The nominal voltage probe input capacity is less than 5.5 pF (the drain connected voltage probe input terminal is not connected to the floating voltage potential, so there is no input capacity impact). As can be seen, the connected voltage probe input capacity is much lower than the MOSFET output capacity, so the minimal impact onto the measured transient state can be supposed.

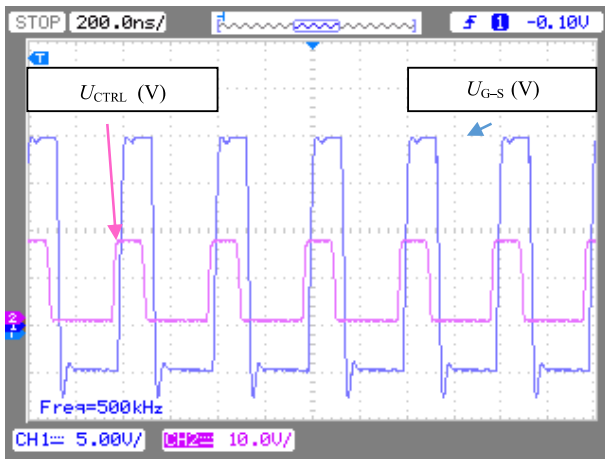


Fig. 7: Driver prototype response, no voltage at the power circuit, input driver signal voltage 1:1 (V) - violet curve, reached G-S voltage directly on the power transistor 1:1 (V) - blue curve.

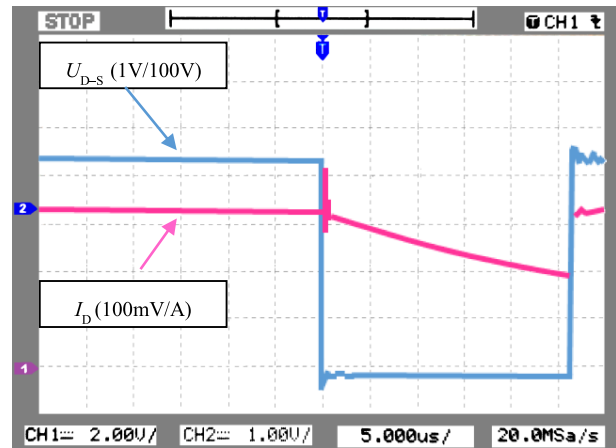


Fig. 9: Obtained one-pulse switching process at  $U_{IN} = 1000$  V, drain-source voltage 1:100 (V) - blue curve, drain current 100 mV/A (V) - violet curve.

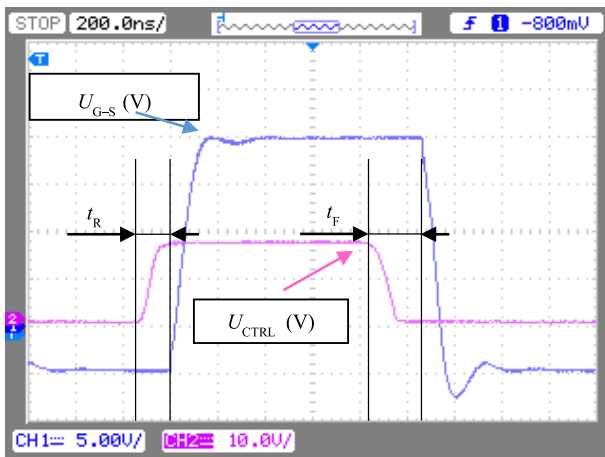


Fig. 8: Detailed driver prototype response, no voltage at the power circuit, input driver signal voltage 1:1 (V) - violet curve, reached G-S voltage directly on the power transistor 1:1 (V) - blue curve.

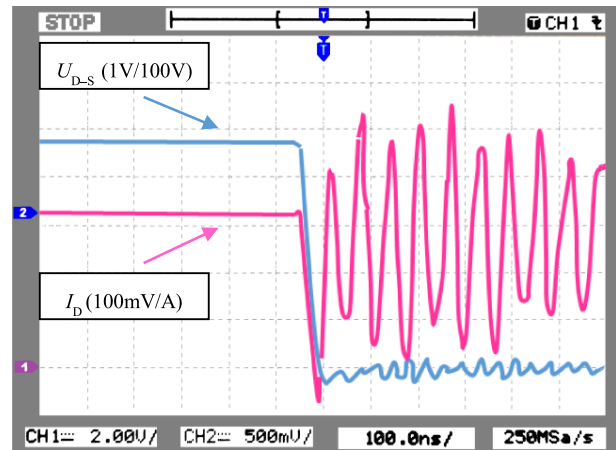
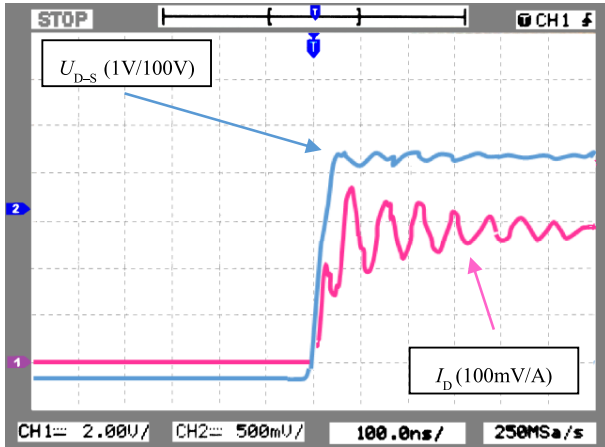


Fig. 10: Obtained switching-on process detail at  $U_{IN} = 1000$  V - drain-source voltage 1:100 (V) - blue curve, drain current 100 mV/A (V) - violet curve.

It is important not to exceed the switched MOSFET absolute maximum rating, which is passed, but the final overshoots are different because of the reverse transfer capacitance impact, see Fig. 12 and Fig. 13.

The responses measured via the probes mentioned in App. A and App. B are shown in Fig. 9, Fig. 10, Fig. 11, Fig. 12, and Fig. 13. The nominal output

The proposed prototype was tested via one-pulse, which occurred for 25  $\mu$ s. The switching pulse process can be seen in Fig. 9, where the drain-source voltage falls down at the beginning of the switching-on process, and the drain current flowing through the  $RL$  load begins exponentially growing up at the same time. This is in progress until the beginning of the switching-off process, when the drain current falls down to zero and the drain-source voltage grows to  $U_{IN}$  value over the switching-off overshoot.



**Fig. 11:** Obtained switching off process detail at  $U_{IN} = 1000$  V - drain-source voltage 1:100 (V) - blue curve, drain current 100 mV/A (V) - violet curve.

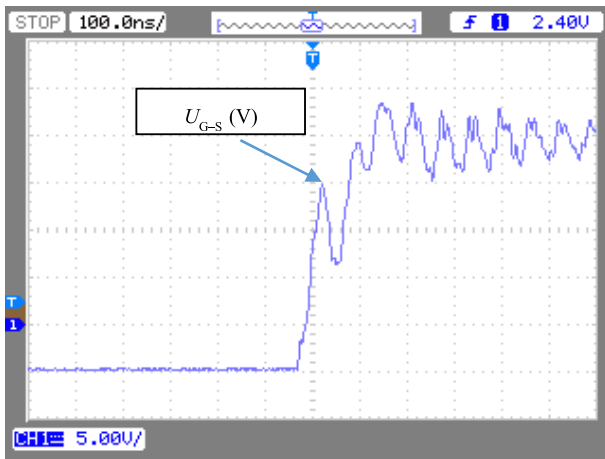


**Fig. 12:** Obtained switching on process detail at  $U_{IN} = 1000$  V - gate-source voltage measured directly on power transistor (V).

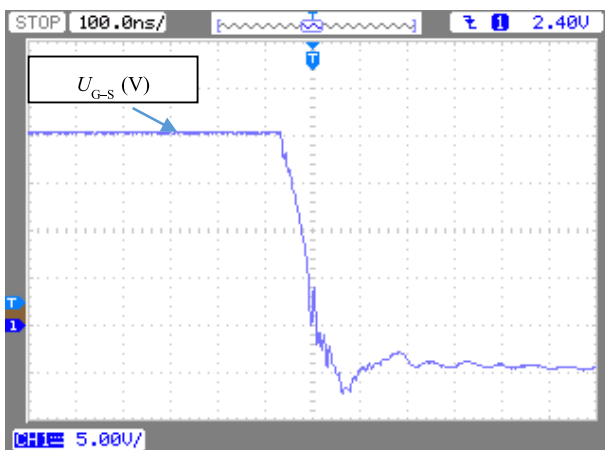


**Fig. 13:** Obtained switching off process detail at  $U_{IN} = 1000$  V, gate-source voltage measured directly on power transistor (V).

The highly smoothed quasi-periodic multi-harmonics drain current oscillations can be observed within

the scoped curves, see Fig. 10 and Fig. 11, which represent the details of the switching-on and switching-off processes. These oscillations are caused by a parasitic LC circuit generated by the inductance of the wires between the power MOSFET source and the load and by the P-N junction capacity of the load diode  $D_L$  (see Fig. 6).

However, the drain current oscillates shortly after the switching-on process is over, but the power transistor perfectly switches-on with no oscillations within the switching process. It can be seen in Fig. 10 from the curve of the drain-source voltage, which oscillates slightly near the steady state voltage drop value.

The obtained rise time in Fig. 10 is approx. 40 ns, which is close to the nominal value of 20 ns. The nominal turn-on delay is 65 ns. The used voltage probe rise time is less than 14 ns, which demonstrates the possibility of monitoring this curve correctly by the probe.

The drain current quasi-periodic oscillations can be also observed at the switching off-process, see Fig. 11, but the drain-source voltage curve rises continuously, within 20 ns, which is close to the nominal fall time of 18 ns.

Figure 12 and Fig. 13 show the gate-source voltage measured within the same switching-on and switching-off process, respectively, as it is reflected within Fig. 10 and Fig. 11. Some transpositions of the drain current oscillations to the gate-source voltage, can be observed there, see Fig. 12 and Fig. 13.

However, the overshoot of the rising slope does not exceed 25 V, which is the applied MOSFET absolute maximum rating, see Fig. 12.

The falling slope within the switching-off process does not exceed -10 V, which is the used MOSFET absolute maximum rating, see Fig. 13.

## 5. Conclusion

A new SiC MOSFET driver is presented in the paper. It was discovered that the tuned up realized driver prototype is able to rich the nominal values of rise and fall times of the assigned controlled power transistor, even though there was no effort to localize the driver as close as possible to the controlled transistor. The approx. 20 cm long coaxial cable was used in this case. Despite the related wire inductance, the used MOSFET gate-source voltage absolute maximum ratings were not exceeded. The steady states gate-source voltages were set to the transistor recommended values.

The obtained results are very beneficial from the practical point of view, because it is not usually possible to locate the driver absolutely

near the driven power transistor according to the converter construction aspects. The proposed solution enables to work near the transistor limits and also with the use of a cable between the driver and the power transistor.

The suppressed current oscillations can be observed at the ends of the switching processes. These are originated by the response of the parasitic  $LC$  element of the testing circuit. Although these oscillations are transferred onto gate-source voltage, the switching processes are continuous, which can be seen from the curves of the drain-source voltage.

## Acknowledgment

This work was supported by the Student Grant Competition of VSB–Technical University of Ostrava under project SP2021/70 and by the Ministry of Education, Youth and Sports of the Czech Republic under project LTE220001 - E-Town. Also, we would like to thank to Mr. Petr Malcok from SIEMENS company for his support and cooperation.

## Author Contributions

J.S. and V.D. created the conceptualization and formulated the main ideas of the proposed device including the application requirements leading to the main goals. M.S. and D.K. prepared the prototype design and worked cooperating with V.D. within the prototype building-up process. J.B. and M.S. performed testing and final tuning up the prototype to get the presented obtained results. D.K. and J.B. performed the state of the art investigation and J.S. performed the critical verification of the obtained results and wrote the paper draft including the original draft preparation, and editing.

## References

- [1] SABRI, S., E. VAN BRUNT, A. BARKLEY, B. HULL, M. O'LOUGHLIN, A. BURK, S. ALLEN and J. PALMOUR. New generation 6.5 kV SiC power MOSFET. In: *2017 IEEE 5th Workshop on Wide Bandgap Power Devices and Applications (WiPDA)*. Albuquerque: IEEE, 2017, pp. 246–250. ISBN 978-1-5386-3117-1. DOI: 10.1109/WiPDA.2017.8170555.
- [2] FRIVALDSKY, M., M. PIPISKA and P. SOJKA. Evaluation of switching performance of Si, SiC and GaN power transistors within ZVS mode. In: *2019 International Conference on Electrical Drives & Power Electronics (EDPE)*. The High Tatras: IEEE, 2019, pp. 30–35. ISBN 978-1-72810-389-1. DOI: 10.1109/EDPE.2019.8883902.
- [3] ZHAO, T., J. WANG, A. Q. HUANG and A. AGARWAL. Comparisons of SiC MOSFET and Si IGBT Based Motor Drive Systems. In: *2007 IEEE Industry Applications Annual Meeting*. New Orleans: IEEE, 2007, pp. 331–335. ISBN 978-1-4244-1259-4. DOI: 10.1109/07IAS.2007.51.
- [4] HAZRA, S., A. DE, L. CHENG, J. PALMOUR, M. SCHUPBACH, B. A. HULL, S. ALLEN and S. BHATTACHARYA. High Switching Performance of 1700V, 50A SiC Power MOSFET over Si IGBT/BiMOSFET for Advanced Power Conversion Applications. *IEEE Transactions on Power Electronics*. 2015, vol. 31, iss. 7, pp. 4742–4754. ISSN 1941-0107. DOI: 10.1109/TPEL.2015.2432012.
- [5] CHEN, Y., J. DU, L. FENG, J. XIAO, J. ZHANG and Y. HE. Comparative Study on Driving Switching Characteristics of GaN-FET and SiC-MOSFET in Transient High Voltage Pulse Discharge Circuit. In: *2020 IEEE International Conference on High Voltage Engineering and Application (ICHVE)*. Beijing: IEEE, 2020, pp. 1–4. ISBN 978-1-72815-511-1. DOI: 10.1109/ICHVE49031.2020.9279479.
- [6] TANG, T. and C. BURKHART. Hybrid MOSFET/driver for ultra-fast switching. *IEEE Transactions on Dielectrics and Electrical Insulation*. 2009, vol. 16, iss. 4, pp. 967–970. ISSN 1558-4135. DOI: 10.1109/TDEI.2009.5211841.
- [7] PERDUKOVA, D., P. FEDOR, V. FEDAK and S. PADMANABAN. Lyapunov Based Reference Model of Tension Control in a Continuous Strip Processing Line with Multi-Motor Drive. *Electronics*. 2019, vol. 8, iss. 1, pp. 1–23. ISSN 2079-9292. DOI: 10.3390/electronics8010060.
- [8] LI, Y. H. and V. R. K. KANAMARLAPUDI. A Generic Gate Driver for SiC MOSFETs with adjustable Positive and Negative Rail Voltage. In: *2018 Asian Conference on Energy, Power and Transportation Electrification (ACEPT)*. Singapore: IEEE, 2018, pp. 1–5. ISBN 978-1-5386-8136-7. DOI: 10.1109/ACEPT.2018.8610828.
- [9] NAYAK, P., M. V. KRISHNA, K. VASUDEVAKRISHNA and K. HATUA. Study of the effects of parasitic inductances and device capacitances on 1200 V, 35 A SiC MOSFET based voltage source inverter design. In: *2014 IEEE International Conference on Power Electronics, Drives and Energy Systems (PEDES)*. Mumbai:

- IEEE, 2014, pp. 1–6. ISBN 978-1-4799-6373-7. DOI: 10.1109/PEDES.2014.7042035.
- [10] ANTHON, A., J. C. HERNANDEZ, Z. ZHANG and M. A. E. ANDERSEN. Switching investigations on a SiC MOSFET in a TO-247 package. In: *IECON 2014 - 40th Annual Conference of the IEEE Industrial Electronics Society*. Dallas: IEEE, 2014, pp. 1854–1860. ISBN 978-1-4799-4032-5. DOI: 10.1109/IECON.2014.7048754.
- [11] YI, P., Y. CUI, A. VANG and L. WEI. Investigation and evaluation of high power SiC MOSFETs switching performance and overshoot voltage. In: *2018 IEEE Applied Power Electronics Conference and Exposition (APEC)*. San Antonio: IEEE, 2018, pp. 2589–2592. ISBN 978-1-5386-1180-7. DOI: 10.1109/APEC.2018.8341382.
- [12] ROTHMUND, D., D. BORTIS and J. W. KOLLAR. Highly Compact Isolated Gate Driver With Ultrafast Overcurrent Protection for 10 kV SiC MOSFETs. *CPSS Transactions on Power Electronics and Applications*. 2018, vol. 3, iss. 4, pp. 278–291. ISSN 2475-742X. DOI: 10.24295/CPSSTPEA.2018.00028.
- [13] ZHANG, J., H. WU, J. ZHAO, Y. ZHANG and Y. ZHU. A Resonant Gate Driver for Silicon Carbide MOSFETs. *IEEE Access*. 2018, vol. 6, iss. 1, pp. 78394–78401. ISSN 2169-3536. DOI: 10.1109/ACCESS.2018.2885023.
- [14] IYENGAR, P., T. C. LIM, S. J. FINNEY, B. W. WILLIAMS and M. A. SINCLAIR. Design and analysis of an enhanced MOSFET gate driver for pulsed power applications. *IEEE Transactions on Dielectrics and Electrical Insulation*. 2013, vol. 20, iss. 4, pp. 1136–1145. ISSN 1558-4135. DOI: 10.1109/TDEI.2013.6571428.
- [15] THEODORIDIS, M. P. and S. V. MOLLOV. Robust MOSFET Driver for RF, Class-D Inverters. *IEEE Transactions on Industrial Electronics*. 2008, vol. 55, iss. 2, pp. 731–740. ISSN 1557-9948. DOI: 10.1109/TIE.2007.896137.
- [16] SUKHATME, Y., V. K. MIRYALA, P. GANESAN and K. HATUA. Digitally Controlled Gate Current Source-Based Active Gate Driver for Silicon Carbide MOSFETs. *IEEE Transactions on Industrial Electronics*. 2020, vol. 67, iss. 12, pp. 10121–10133. ISSN 1557-9948. DOI: 10.1109/TIE.2019.2958301.
- [17] CHENNU, J. V. P. S., R. MAHESHWARI and H. LI. New Resonant Gate Driver Circuit for High-Frequency Application of Silicon Carbide MOSFETs. *IEEE Transactions on Industrial Electronics*. 2017, vol. 64, iss. 10, pp. 8277–8287. ISSN 1557-9948. DOI: 10.1109/TIE.2017.2677307.
- [18] YANG, Y., Y. WEN and Y. GAO. A Novel Active Gate Driver for Improving Switching Performance of High-Power SiC MOSFET Modules. *IEEE Transactions on Power Electronics*. 2019, vol. 34, iss. 8, pp. 7775–7787. ISSN 1941-0107. DOI: 10.1109/TPEL.2018.2878779.
- [19] ZHANG, Z., K. YAO, G. KE, K. ZHANG, Z. GAO, Y. WANG, X. REN and Q. CHEN. SiC MOSFETs Gate Driver With Minimum Propagation Delay Time and Auxiliary Power Supply With Wide Input Voltage Range for High-Temperature Applications. *IEEE Journal of Emerging and Selected Topics in Power Electronics*. 2020, vol. 8, iss. 1, pp. 417–428. ISSN 2168-6785. DOI: 10.1109/JESTPE.2019.2951358.
- [20] DYMOND, H. C. P., J. J. O. DALTON and B. H. STARK. Rapid Co-Optimisation of Turn-On and Turn-Off Gate Resistor Values in DC:DC Power Converters. In: *2018 IEEE Energy Conversion Congress and Exposition (ECCE)*. Portland: IEEE, 2018, pp. 5357–5364. ISBN 978-1-4799-7312-5. DOI: 10.1109/ECCE.2018.8558406.

## About Authors

**Jan STROSSA** was born in Prague, Czech Republic. He received his M.Sc. degree in Applied Electronics from the VSB–Technical University of Ostrava in 2018. He is currently a Ph.D. student at the Department of Electronics, Faculty of Electrical Engineering and Computer Science, VSB–Technical University of Ostrava, and works for Siemens Mobility Austria, GmbH, R&D at the same time. His research interests include power electronics in the field of soft switching multiport DC-DC converters.

**Vladislav DAMEC** was born in Karvina, Czech Republic. He received the M.Sc. and Ph.D. degrees in Electronics and Electrical machines, apparatus and drives from VSB–Technical University of Ostrava, Czech Republic, in 2000 and 2003, respectively. He works currently for Siemens Mobility Austria, GmbH, R&D and as an assistant professor at Department of Electronics by VSB–Technical University of Ostrava at same time. His research interests include power electronics in the field of large electric drives.

**Martin SOBEK** was born in Frydek-Mistek, Czech Republic, in 1983. He received the M.Sc. and Ph.D. degrees in Electronics and Electrical machines, apparatus and drives from VSB–Technical University of Ostrava, Czech Republic, in 2008 and 2012, respectively. He works currently as an assistant professor

at Department of Electronics by VSB–Technical University of Ostrava. His current research interests are microprocessor control systems, digital electronics, power electronics and electric drives.

**Daniel KOURIL** was born in Ostrava, Czech Republic. He received his M.Sc. degree in Applied Electronics from the VSB–Technical University of Ostrava in 2017. His research focused on the Hardware development of a modern processor control systems in the field of electric controlled drives for the use with GA and ANN-based algorithms.

**Jakub BACA** was born in Frydek-Mistek, Czech Republic. He received his M.Sc. in Applied Electronics from the VSB–Technical University of Ostrava in 2017. He is currently a Ph.D. student at the Department of Electronics, Faculty of Electrical Engineering and Computer Science, VSB–Technical University of Ostrava. His main research interest is currently focused on artificial neural networks and their use in the field of electric drives, especially for sensorless control of induction machine drives.

## Appendix A Used Drain Current Probe

LEM PR50

- Bandwidth  $f_{BW} = 50$  MHz.
- Rise time  $t_r < 7$  ns.
- Delay time  $t_d < 25$  ns.

## Appendix B Used Drain-Source Voltage Probe

Teledyne LeCroy AP031

- Bandwidth  $f_{BW} = 25$  MHz.
- Rise time  $t_r < 14$  ns.
- Input capacitance  $t_d < 5.5$  pF each input terminal to ground.